

A Comparative Study of the PIV and LDV Measurements on a Self-induced Sloshing Flow

Saga, T.*¹, Hu, H.*¹, Kobayashi, T.*¹, Murata, S.*², Okamoto, K.*³ and Nishio, S.*⁴

*1 Institute of Industrial Science, University of Tokyo, 7-22-1 Roppongi, Minato-ku, Tokyo 106-8558, Japan.
e-mail:saga@iis.u-tokyo.ac.jp or huhui@iis.u-tokyo.ac.jp

*2 Dept. of Mechanical and System Engineering, Kyoto Institute of Technology, Matsugasaki, Sakyo-ku, Kyoto 606-8585, Japan.

*3 Nuclear Engineering Research Laboratory, University of Tokyo, Tokai-mura, Ibaraki, 319-1109, Japan.

*4 Dept. of Maritime Science, Kobe University of Mercantile Marine, Kobe 658-0022, Japan.

Received 24 January 2000.

Revised 19 April 2000.

Abstract: Particle Imaging Velocimetry (PIV) and Laser Doppler Velocimetry (LDV) measurements on a self-induced sloshing flow in a rectangular tank had been conducted in the present study. The PIV measurement result was compared with LDV measurement result quantitatively in order to evaluate the accuracy level of the PIV measurement. The comparison results show that the PIV and LDV measurement results agree with each other well in general for both mean velocity and fluctuations of the velocity components. The average disagreement level of the mean velocity between PIV and LDV measurement results was found to be within 3% of the target velocity for the PIV system parameter selection. Bigger disagreements between the PIV and LDV measurement results were found to concentrate at high shear regions. The spatial resolution and temporal resolution differences of the PIV and LDV measurements and the limited frames of the PIV instantaneous results were suggested to be the main reasons for the disagreement.

Keywords: PIV technique, LDV technique, PIV accuracy evaluation, self-induced sloshing phenomena.

Nomenclature:

b	the height of the test tank inlet, $b = 20$ mm
E	the width of the exit of the test tank
f	the frequency of the self-induced sloshing in the test tank
H	the water level height of the free surface in the test tank
LDV-PIV	the disagreement of the PIV and LDV measurement results
	$LDV - PIV = \sqrt{(U_{LDV} - U_{PIV})^2 + (V_{LDV} - V_{PIV})^2}$
n	The mode of the self-induced sloshing free surface in the test tank
Re	Reynolds Number, $Re = \frac{\rho U_0 b}{\mu} = 6700$ for the present study
r.m.s ($u_{i,j}$), r.m.s ($v_{i,j}$)	fluctuations of the velocity components,

$$r.m.s.(u_{i,j}) = \frac{\sqrt{\sum_{t=1}^N (u_{i,j,t} - U_{i,j})^2}}{N}, \quad r.m.s.(v_{i,j}) = \frac{\sqrt{\sum_{t=1}^N (v_{i,j,t} - V_{i,j})^2}}{N}$$

$T_{i,j}$	in-plane turbulent intensity, $T_{i,j} = \sqrt{(\text{r.m.s.}(u_{i,j}))^2 + (\text{r.m.s.}(v_{i,j}))^2}$
U_0	inlet jet velocity
u, v	the instantaneous velocity components along x, y axial direction
U, V	ensemble averaged velocity
W	the width of the test tank, $W = 300$ mm

Subscripts

i, j	the index of the measurement points along x, y axial direction
LDV	LDV measurement result
Phase	phase averaged values
PIV	PIV measurement result
t	time steps

1. Introduction

As a non-intrusive whole field measuring technique, Particle Imaging Velocimetry (PIV) can offer many advantages for the studying of fluid mechanics over other conventional one-point experimental techniques like Laser Doppler Velocimetry (LDV) or Hot Wire Anemometer (HWA). For example, PIV can reveal the global structures in a two-dimensional or three-dimensional flow field instantaneously and quantitatively without disturbing the flow, which are very useful and necessary for the research of flow mechanism, in particular for the study of unsteady and complex flow phenomena. Due to these advantages, PIV technique has widely been used and rapidly developed in the past two decades.

However, PIV technique is still under development at current state, and there are still a lot of work to be done in order to make PIV technique as a more practical and standardized measurement tool. For example, there is no standard for the effectiveness and accuracy evaluation of a PIV system. This results in that the users of PIV systems had to spend lots of time and costs to learn much know-how and to optimize various parameters for PIV image acquiring and processing to get an accurate velocity field. In order to popularize the PIV technique for practical use, a "PIV-STD" Project is being conducted in Japan to evaluate the effectiveness of PIV technique and to develop PIV standards and guide tools for PIV users.

A typical PIV experiment always includes two steps, which are the PIV image capturing and PIV image processing. For the PIV image processing, "PIV-STD" Project had developed many sets of artificial images, which can be used to evaluate various PIV image-processing algorithms (Okamoto et al., 1997). The artificial images, which were called PIV standard images, had been distributed freely at the INTERNET site <http://www.vsj.or.jp/piv/>.

In order to evaluate the whole performance of a PIV system, the second part of the "PIV-STD" Project, which was named as "PIV standard experiment" sub-project, was also proposed. The same target flow field was measured in 15 research laboratories over Japan and South Korea by using LDV systems and 20 sets of PIV systems with various illumination sources, CCD cameras, particle tracers and image processing algorithms (Kobayashi et al., 1999). PIV system characteristics were evaluated based on the comparison of the measurement results of LDV systems and PIV systems. The present study is just one part of the work under the "PIV standard experiment" sub-project.

For the effectiveness and accuracy level evaluation of PIV result, many studies had been conducted in the past based on the image processing result of artificial images, which were generated artificially with a pre-set velocity distribution, by using various PIV image processing methods or algorithms. By comparison with the velocity distribution obtained through PIV image processing and the pre-set velocity data with the artificial images, the accuracy level of the PIV result was evaluated. Although many important results had been got through these studies, it should be noted that the artificial images used in those researches always have very high image quality, i.e. much better signal to noise ratio (SNR) than the PIV images obtained from actual PIV experiments. Besides PIV image processing, PIV experiment also includes flow field illumination and PIV image capturing, which may affect the PIV final result accuracy as well. Therefore, the accuracy level of a PIV system still can not be predicted successfully just based on the PIV image processing result of those artificial images.

In order to evaluate the accuracy level of whole PIV system, a comparative study of PIV and LDV measurements on a same flow field had been conducted in the present paper. The measurement target flow is a self-induced sloshing flow field in a rectangular tank. The free surface of the fluid (water) in the rectangular tank

oscillates periodically with a constant frequency, which is decided by the eigenvalue of the water in the test tank. The results of the PIV measurement and LDV measurement were compared quantitatively to evaluate the PIV measurement. The compared parameters used in the present study included the frequency of the self-induced sloshing, the ensemble-averaged velocity and fluctuations of the velocity components, phase-averaged velocity and fluctuations of the velocity components. The effect of the sample number of the PIV instantaneous velocity fields and the spatial resolution of the PIV images on the accuracy level of the PIV result were also discussed in the present study.

2. Experimental Setup

2.1. The Target Flow and Experimental Set-up

The target flow used in the present study is a self-induced sloshing flow in a rectangular tank. Figure 1 shows the schematic view of the thin rectangular test tank. Working fluid (water) flowed horizontally into the test tank and flowed out at a bottom centered vertical outlet. It was found that under certain condition of water level in the test tank and inlet jet velocity, the free surface of the fluid (water) in the rectangular tank might oscillate periodically at a constant frequency decided by the eigenvalue of the fluid in the test tank. This phenomenon was called "self-induced sloshing." The characteristics of the self-induced sloshing had been studied by many researchers (Okamoto et al., 1991; Fukuya et al., 1996; Saeki et al., 1998 and Hu et al., 1999). The excitation of the self-induced sloshing was considered to be the non-linear interaction between jet instability and sloshing motion.

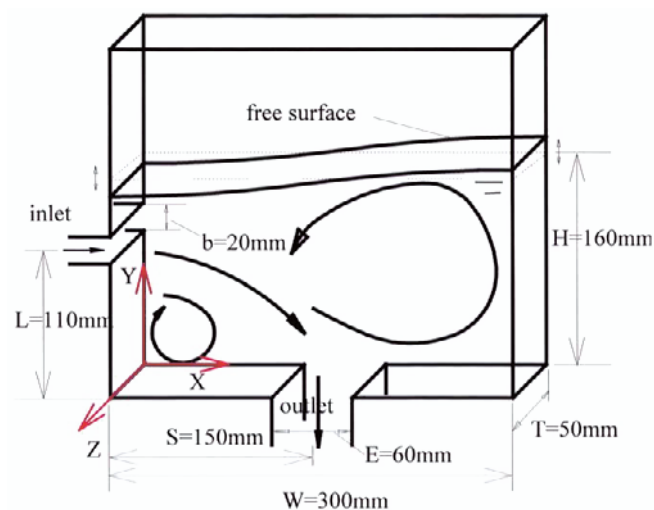


Fig. 1. The schematic of the test tank.

Figure 2 shows the experimental set-up used in the present research. The flow in the test loop was supplied from a head tank, which was continuously pump-filled from a lower tank. The water level in the head tank was maintained constant by an overflow system in order to eliminate the effect of the pump vibration on the inlet condition of the test tank. The flow rate of the flow loop, which was used to calculate the representative velocity and Reynolds numbers, was measured by a flow meter. Convergent unit and honeycomb structures were installed in the upstream of the inlet of the test tank to insure the uniform flow entrance. The flow rate and the water level of the free surface in the test tank was adjustable by changing the position of the valves installed in the flow loop. A water level sensor was used to detect the oscillation of the water free surface in the test tank, which can also generate a signal at the pre-set water free surface level to a Synchronizer Control System to trig the PIV and LDV systems to do phase averaged measurement.

During the experiment, the averaged water level in the test tank was set at about $H = 160$ mm. The flow rate of the test loop was about 20 liter/min, which corresponded to the averaged velocity at the inlet of the test tank (U_0) being about 0.33 m/s, and Reynolds number about $Re = 6700$ based on the averaged velocity and the height of the inlet ($b=20$ mm). Since the test tank was designed to have the flow field in the test tank to be two-dimensional,

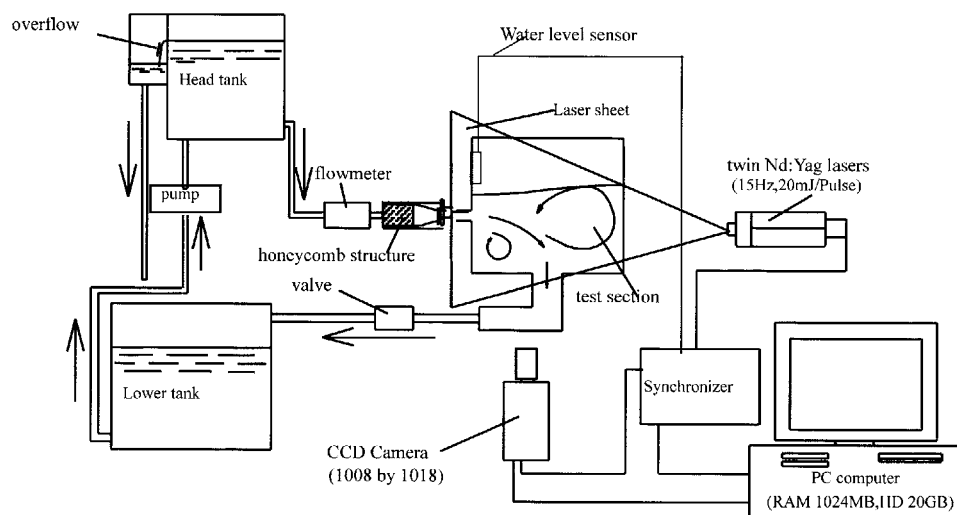


Fig. 2. The schematic of the experimental set-up.

our measurement result also verified that the flow field in the test tank was almost two-dimensional except the regions near the two walls. The comparative measurements of the PIV and LDV systems were conducted at the middle section of the test tank ($Z = 25$ mm section) in the present study.

2.2 PIV System

For the PIV measurement, double pulsed Nd:Yag lasers were used to supply pulsed laser sheet (thickness of the sheet is about 1.0 mm) with the frequency of 7.5 Hz and power of 20 mJ/pulse to illuminate the measured flow field. Polystyrene particles (diameter of the particles is about 20-50 μm , density is 1.02 kg/liter) were used as PIV tracers in the flow field. A 1008 by 1018 pixels Cross-Correlation CCD array camera (PIVCAM 10-30) was used to capture PIV images. The twin Nd:Yag lasers and the CCD camera were controlled by a Synchronizer Control System. The PIV images captured by the CCD camera were digitized by an image processing board, then transferred to a workstation (host computer, CPU 450 MHz, RAM 1024 MB, HD 20 GB) for image processing and displayed on a PC monitor.

In the present PIV measurement, the PIV images with two different spatial resolutions were captured. One is 0.16 mm/pixel (high spatial resolution) and another is 0.32 mm/pixel (low spatial resolution). For the PIV image processing, rather than tracking individual particle, the cross correlation method (Willert and Gharib, 1991) was used to obtain the averaged displacement of the ensemble particles. The images were divided into 32 by 32 pixel interrogation windows, and 50% overlap grids were employed for the PIV image processing. The post-processing procedures, which include sub-pixel interpolation (Hu et al., 1998) and spurious velocity deletion (Westerweel, 1994) were used to improve the accuracy of the PIV result.

The velocity of the inlet jet, which is about 0.4 m/s, was selected as the target velocity for the present PIV system parameter set up. The time interval between two laser pulses was set at 2 ms (high spatial resolution case) and 4 ms (low spatial resolution case). The averaged displacement of the particles in the inlet jet is about 6 pixels between the two laser pulses.

Since the cross-correlation method was used for PIV image processing in the present study, the obtained velocity is the averaged velocity of the particles in the interrogation window. So, the spatial resolution should be the sizes of the interrogation windows. Hence, the spatial resolution of the present PIV measurement is about 5 mm \times 5 mm \times 1 mm for the high spatial resolution PIV image case, and 10 mm \times 10 mm \times 1 mm for the low spatial resolution PIV image case by using 32 by 32 pixel interrogation windows. Since the frequency of the pulsed Nd:Yag lasers was set at 7.5 Hz, the temporal resolution of the present PIV measurement is 3.75 Hz according to the Nyquist critical principle.

2.3 LDV System

The LDV system used in the present study was composed by an Argon Laser (1.5 W), a LDV optical unit (TSI TRCF2), a signal processing system (TSI IFA750) and a Synchronizer Control System (TSI Datalink DL4). Polystyrene particles with the diameter of 1 μm and density of 1.02 kg/liter were used as tracers for the LDV measurement. 30000 data obtained at about 30 seconds were used for the mean velocity and fluctuation of the velocity calculation at every point. The spatial resolution of the present LDV system is about 65.3 μm (volume diameter) \times 0.68 mm (volume length). Since the sample rate of the LDV measurement was set as 1000 Hz, the temporal resolution of the LDV measurement is 500 Hz according to the Nyquist critical principle.

3. Results and Discussions

3.1 Oscillation Frequency of the Self-induced Sloshing

Figure 3 shows the oscillation of the water free surface in the test tank with time at three different locations, i.e., left side (inlet side), center and right side of the test tank. The frequency of the self-induced sloshing of the water free surface can be calculated from these signals, which is 1.6 Hz.

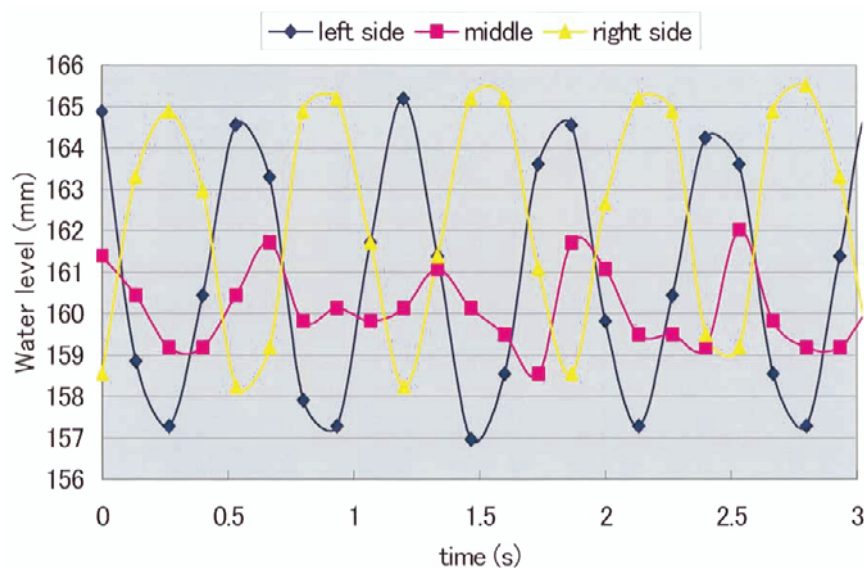


Fig. 3. The oscillation of the water free surface in the test tank.

According to the research of Fukaya et al. (1996), the self-induced sloshing mode of the present study is the first sloshing mode. Okamoto et al. (1991) had suggested that the frequency of the self-induced sloshing equals to the eigenvalue of the water in the test tank, which can be expressed as:

$$f^n = \frac{1}{2\pi} \sqrt{\frac{n\pi g}{W} \tanh\left(\frac{n\pi H}{W}\right)} \quad (1)$$

where n is the mode number of the sloshing, W is the width of the test tank and H is the water level height of the water in the test tank.

By using above equation, the first mode eigenvalue of the water in the test tank for the present study can be calculated, which is 1.56 Hz. The difference between the frequency of the self-induced sloshing measured by present study ($f = 1.6$ Hz) and the first mode eigenvalue of the water in the test tank given by Eq. (1) is within 3%, which verified the result of Okamoto et al. (1991).

Figure 4 shows typical instantaneous velocity distributions from the PIV measurement at two time steps. 1000 frames of such instantaneous velocity fields were captured in the present PIV measurement with the rate of 7.5 Hz. Besides the two big circulation regions at the right side and left lower corner of the test tank (which are steady), a smaller vortex (which is unsteady) can also be found in the PIV instantaneous velocity fields, which shed from the inlet jet periodically. The whole flow field in the test tank, such as the path of the inlet jet to the exit, the

size of the two circulation regions, and the flow direction at the exit of the test tank, changed very drastically with the evolution of this unsteady vortex. By using these instantaneous velocity data, the power spectrum of the velocity (u and/or v components) can be calculated through FFT transformation, which is shown in Fig. 5(a) for the velocity u -component. The power spectrum of the velocity (u -component) at the same point by LDV measurement is shown in Fig. 5(b). Although the temporal resolution and the sample numbers of the PIV and LDV measurement results are different, both the PIV and LDV measurements can identify the frequency of the self-induced sloshing well with an obvious peak at 1.6 Hz in the power spectrum profiles.

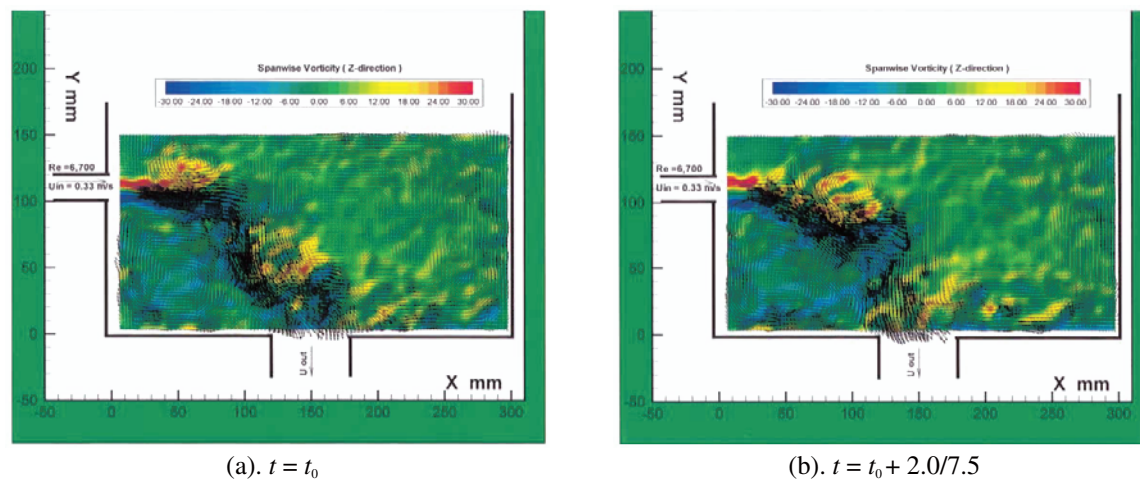
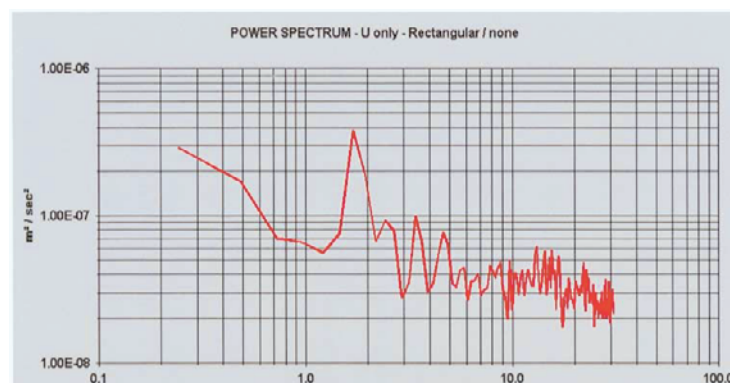
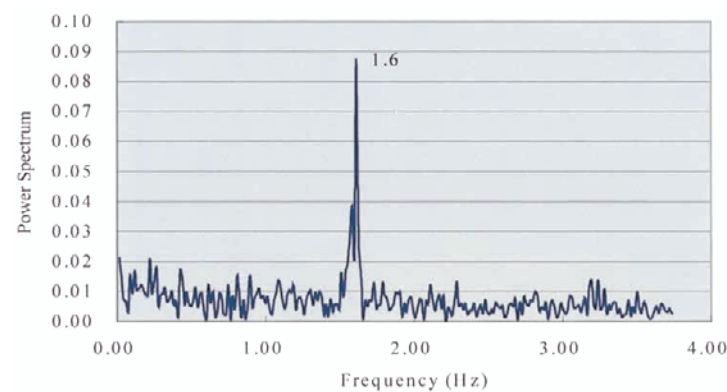


Fig. 4. Typical PIV instantaneous velocity fields.



(a) PIV result



(b) LDV result

Fig. 5. The velocity power spectrum (u -component) at the point ($X = 100$ mm, $Y = 110$ mm, $Z = 25$ mm).

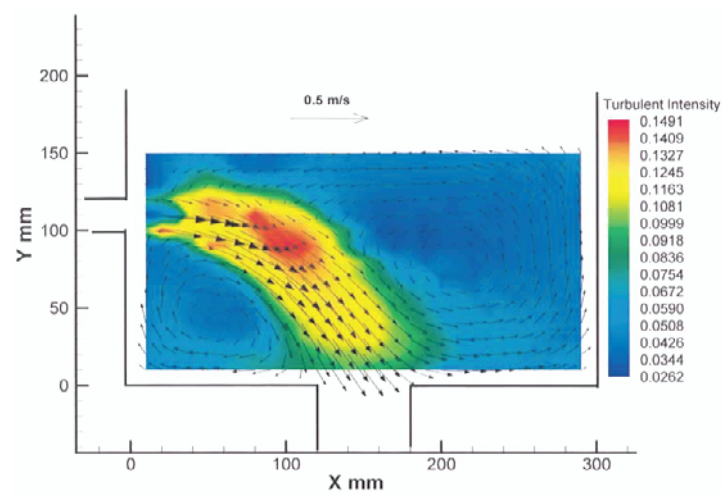
3.2 Ensemble-averaged Velocity and Fluctuations of the Velocity Components

In the present study, 1000 frames of the instantaneous PIV velocity frames obtained by the PIV system at the rate of 7.5 Hz and 30000 samples at each point got by LDV system at the data rate of 1000 Hz were used to calculate the ensemble-averaged values of the flow field.

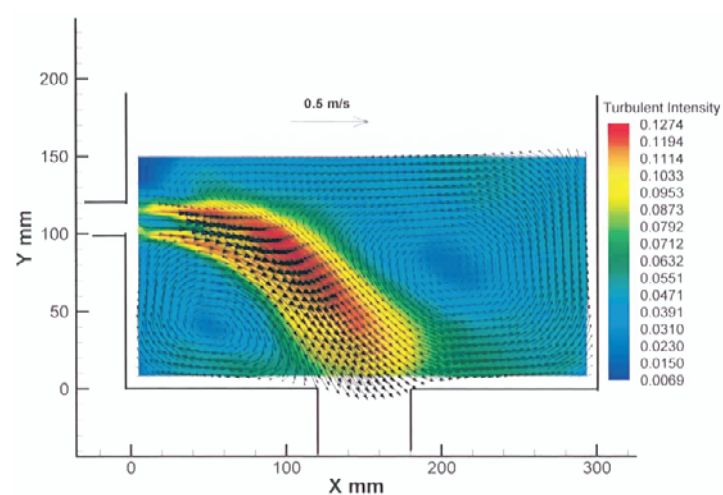
Figure 6 shows the ensemble-averaged velocity fields and the in-plane turbulent intensity (T_{ij}) distributions in the test tank from the PIV and LDV measurement results. In the ensemble-averaged velocity fields, only two big circulation regions can be found at the right side and the left lower corner of the test tank. The unsteady vortex revealed in the above instantaneous flow fields, which shed periodically from the inlet jet, cannot be found in the ensemble-averaged velocity distributions. However, the high turbulent intensity region can be found along the shedding path of the unsteady vortex.

It can also be seen that the flow pattern in the test tank revealed by PIV and LDV measurement results is very similar with each other. In order to give a more quantitative comparison of the PIV and LDV measurement results, the ensemble averaged velocity and fluctuations of the velocity components along the inlet central line of the test tank from the PIV and LDV measurements are shown in Fig. 7.

Since the system parameter selection of the present PIV measurement were based on the velocity of the inlet jet flow (target velocity), which is about 0.4 m/s, 3% margin of the target velocity (0.4 m/s) was also shown in Fig. 7(a) for the PIV measurement results. It can be seen that, the PIV result agreed with LDV result well in general for



(a) LDV result



(b) PIV result

Fig. 6. Ensemble-averaged velocity fields and in-plane turbulent intensity distributions.

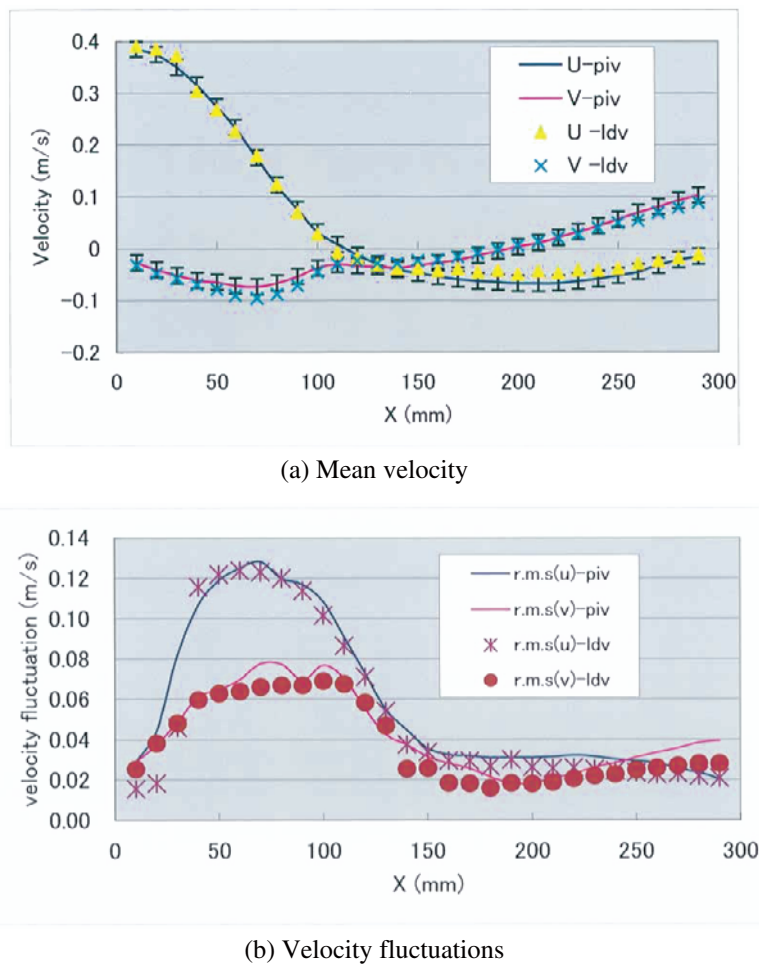


Fig. 7. The comparisons of the ensemble-averaged velocity and velocity fluctuations along the inlet central line of the test tank.

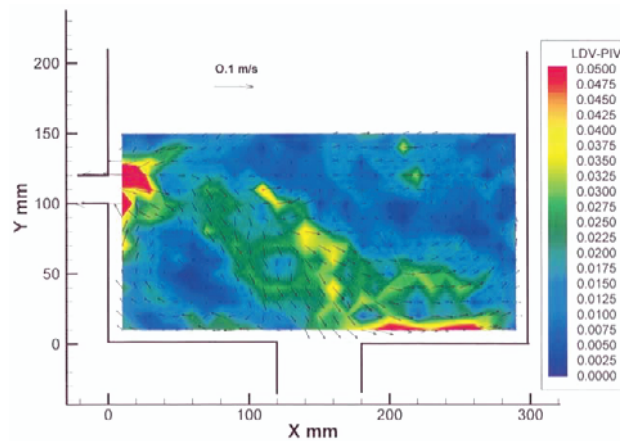
both the ensemble-averaged velocity and velocity fluctuations. The averaged disagreement of the PIV and LDV results for the ensemble-averaged velocity is within 3% of the target velocity. However, some bigger disagreements (always in the high shear region) between the PIV and LDV results can also be found in the profiles (especially for the velocity fluctuation profiles shown in Fig. 7(b)). These may be caused by the different spatial and temporal resolutions of the PIV and LDV measurement results, and the effect of the different spatial resolution of the PIV and LDV measurements will be more serious in the high shear regions. As the spatial resolution of the PIV measurement result improving, the disagreement between the PIV and LDV measurement results is expected to be decreased, which will be verified from Fig. 8.

It should also be noted that the disagreement between the PIV and LDV results is more serious in the velocity fluctuation profiles (Fig. 7(b)) than that in the mean velocity profiles (Fig. 7(a)). This may be explained by that, according to the research of Ullum et al. (1997), the necessary sampling number to calculate the velocity fluctuations should be the square of the number to calculate the mean velocity in order to get the same level of the standard deviation. Hence, the standard deviation by using the same sample number (1000 instantaneous velocity fields) to calculate the velocity fluctuations was expected to be bigger than that to calculate the mean velocity.

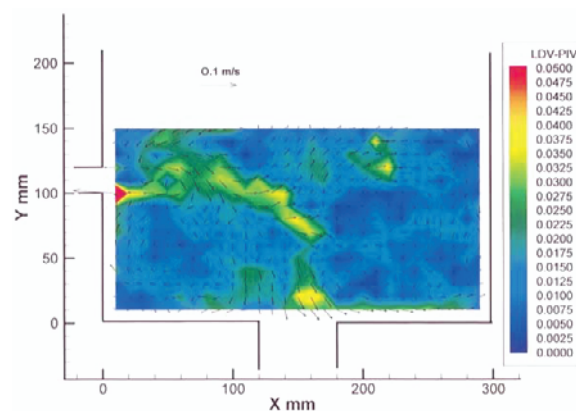
3.3 The Effect of the PIV Image Spatial Resolution

As mentioned above, the PIV images with two different spatial resolution levels had been captured in the present study. Figure 8 shows the disagreement distributions of the LDV measurement result and PIV measurement results (LDV-PIV) using these two kinds of PIV images with different spatial resolutions.

Although the averaged disagreement level of the LDV and PIV results in the whole flow field is about 3% of the target velocity, some bigger disagreements between the LDV and PIV results can still be found in the flow



(a) Low spatial resolution case (0.32 mm/pix)



(b) High spatial resolution case (0.16 mm/pix)

Fig. 8. The effect of the PIV image spatial resolution.

field, which concentrated at the high shear regions. As the PIV image spatial resolution increasing, the sizes of the regions with bigger disagreement values decreased.

3.4 Phase-averaged Velocity and Fluctuations of the Velocity Components

Since the free surface of the water in the test tank oscillated periodically with the frequency of 1.6 Hz, the phase-averaged measurement by using the PIV and LDV systems had also been conducted in the present study. For the phase-averaged measurement, the free surface water level at the left side (inlet side) was detected by a water-level detecting sensor (Fig. 2), which can send a signal to the Synchronizer Control System to trigger the PIV and LDV systems. The PIV phase-averaged velocity distributions from 250 cycle of self-induced sloshing at four phase angles ($\theta = 0, \pi/2, \pi$ and $3\pi/2$) are shown in Fig. 9. The water levels of the free surface at the left side (inlet side) of the test tank were at its highest position, middle level (the free surface level is decreasing), lowest position and middle level (the free surface level is increasing) corresponding to the four phase angles.

Unlike above ensemble-averaged results, which can just reveal two big circulation regions in the flow field, an unsteady vortex can also be visualized clearly in the flow field from the phase-averaged measurement results. The unsteady vortex was found to change its position with the changing of the phase angles. When the phase angle increased from 0 to π , i.e., the free surface water level at the left side of the test tank decreased from its highest position to its lowest position (from Fig. 9(a), Fig. 9(b) to Fig. 9(c)). The unsteady vortex shed from the inlet jet and moved downstream. When the phase angle increased from π to 2π , i.e., the free surface water level at the left side of the test tank began to increase from its lowest position to its highest position (from Fig. 9(c), Fig. 9(d) to Fig. 9(a)). The unsteady vortex was engulfed by the steady circulation region at the right side of the test tank, and another new vortex was found to roll up from the inlet of the test tank. Then, another new self-induced sloshing cycle began.

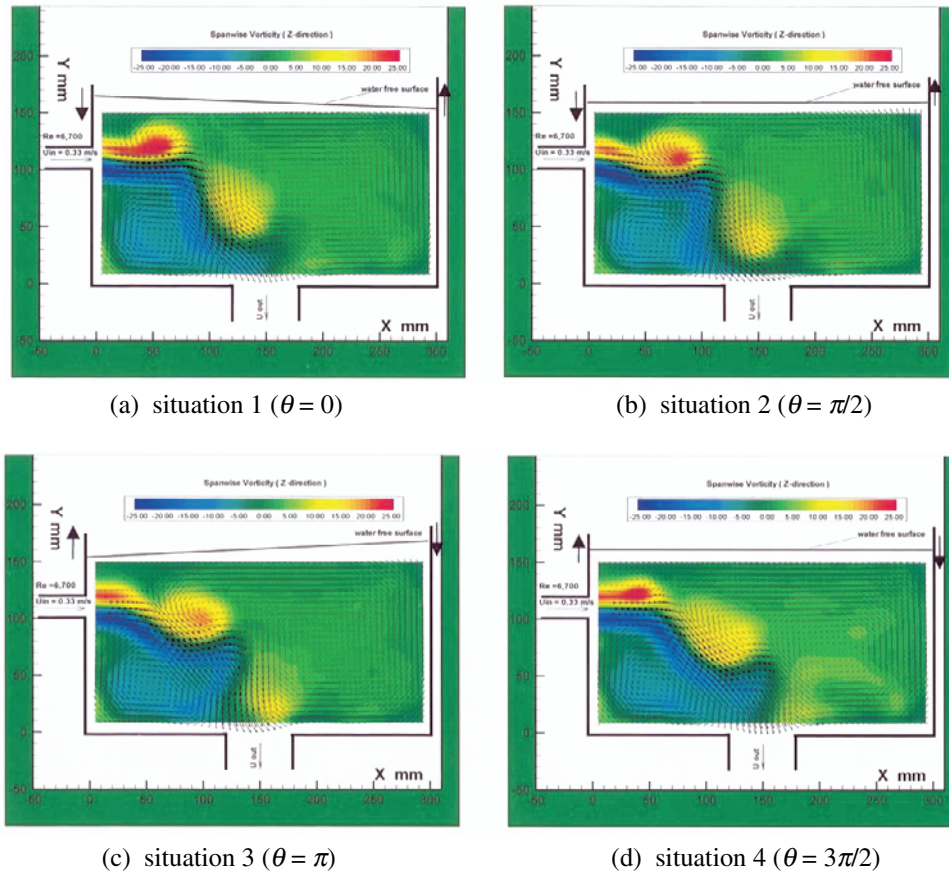
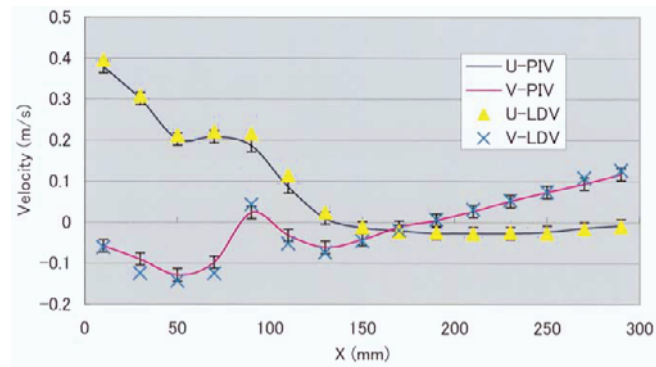
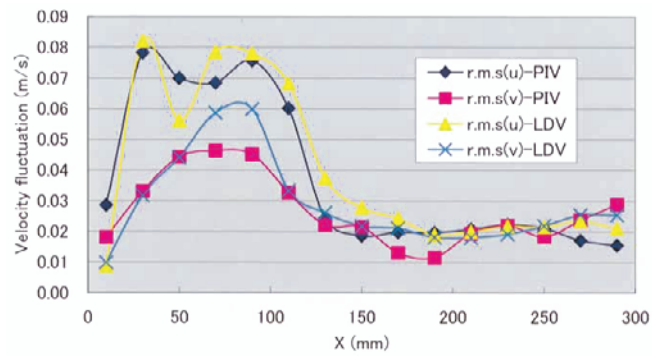


Fig. 9. The phase averaged results of the PIV measurement.



(a) Phase-averaged velocity



(b) Velocity fluctuations

Fig. 10. The comparisons of the phase-averaged values along the inlet central line of test tank (phase angle = $\pi/2$).

Figure 10 shows the phase-averaged velocity and velocity fluctuations along the inlet central line of the test tank from the PIV and LDV measurement results at the phase angle of $\pi/2$. Same as the ensemble-averaged results shown in Fig. 7, the PIV and LDV measurement results agreed with each other well in general. For the phase averaged velocity, the disagreement of PIV and LDV was also found to be within 3% of the target velocity. However, the disagreement of the velocity fluctuations (especially in the high shear region) between the PIV and LDV results was found to be more serious than its ensemble-averaged counterpart (Fig. 7(b)), which may be caused by the fewer sample number for the phase-averaged values ($N = 250$ frames) than that for the ensemble averaged values ($N = 1000$ frames).

4. Conclusions

A comparative study of Particle Imaging Velocimetry (PIV) and Laser Doppler Velocimetry (LDV) measurements on a self-induced sloshing flow in a rectangular tank had been conducted in the present study. The PIV measurement result was compared with LDV measurement result quantitatively in order to evaluate the accuracy level of the PIV measurement result. The comparison results show that the PIV and LDV results agree with each other well in general for both the mean velocity and velocity fluctuations. The disagreement level of the mean velocity between the PIV and LDV results is within 3% of the target velocity. Bigger disagreement regions were found to concentrate at high shear regions. The spatial resolution and temporal resolution differences and the limited frame number of the PIV measurement result were suggested to be the main reasons for the disagreements.

Acknowledgments

The authors wish to thank Mr. Shigeki Segawa at the Institute of Industrial Science, University of Tokyo, Mr. Masaho Nagoshi and Mr. Taizo Higashiyama of KANOMAX JAPAN, INC for their help in conducting the present study.

References

- Fukaya, M., Madarame, H. and Okamoto, K., Growth Mechanism of Self-induced Sloshing Caused by Jet in Rectangular Tank (2nd Report, Multi-mode Sloshing Caused by Horizontal Rectangular Jet), *Trans. of JSME, (B)*, Vol. 62, No. 599 (1996), 64-71.
- Hu, H., Saga, T., Kobayashi, T., Okamoto, K. and Taniguchi, N., Evaluation of the Cross Correlation Method by Using PIV Standard Images, *Journal of Visualization*, Vol.1, No.1 (1998), 87-94.
- Hu, H., Kobayashi, T., Saga, T., Segawa, S., Taniguchi, S., Nagoshi, M. and Okamoto, K., A PIV Study on the Self-induced Sloshing in a Tank with Circulating Flow, *Proceedings of the 2nd Pacific Symposium on Flow Visualization and Image Processing*, (CD-ROM paper No. PF152), (Hawaii, USA), (1999-4).
- Kobayashi, T., Saga, T., Nishio, S. and Okamoto, K., Measurement on a Self-induced Flow by Using Various PIV Systems, *Proceedings of 3rd International Workshop on PIV*, (Santa Barbara, USA), (1999-9), 183-188.
- Okamoto, K., Nishio, S., Kobayashi, T. and Saga, T., Standard Images for Particle Imaging Velocimetry, *Proceedings of the Second International Workshop on PIV*, (Fukui, Japan), (1997-7).
- Okamoto, K., Madarame, H. and Hagiwara, T., Self-induced Oscillation of Free Surface in a Tank with Circulating Flow, C416/092, *IMEchE* (1991), 539-545.
- Saeki, S., Madarame, H., Okamoto, K. and Tanaka, N., Numerical Study on the Growth Mechanism of Self-induced Sloshing Caused by Horizontal Plane Jet, *Proceedings of ASME FED Summer Meeting* (CD-ROM, Paper No. FEDSM98-5208), (Washington D.C., USA), (1998-5).
- Ullum, U., Schmidt, J. J., Larsen, P. S., and McClusky, D. R., Statistical Analysis and Accuracy of PIV Data, *Proceedings of the Second International Workshop on PIV*, (Fukui, Japan), (1997-7).
- Willert, C. E. and Gharib, M., Digital Particle Image Velocimetry, *Experiments in Fluids*, Vol. 10 (1991), 181-199.
- Westerweel, J., Efficient Detection of Spurious Vectors in Particle Image Velocimetry Data, *Experiments in Fluids*, Vol. 16 (1994), 236-247.

Author Profile

Tetsuo Saga: He works in the Institute of Industrial Science, University of Tokyo. His research field is mechanical engineering. Flow visualization and its image analysis, prediction and control of flow induced vibration, automobile aerodynamics are his main research works. His current research interests are in micro- and bio-flow analysis by using PIV.



Hui Hu: He received his Ph. D degree in 1996 from Beijing University of Aeronautics and Astronautics (BUAA), then worked as a Research Fellow of Japan Society for Promotion of Science (JSPS) (1997-1999) in the University of Tokyo. He is a Research Fellow in the Kobayashi Laboratory of Institute of Industrial Science (IIS), University of Tokyo. His current research interests include development new optical diagnostic techniques for fluid flow and heat transfer, which include conventional 2-D PIV technique, 3-D stereoscopic PIV technique and Planar LIF technique. He has also intensive interests in active and passive control of the fluid flow, lobed mixer/ejector exhaust system and gas turbine machinery



Toshio Kobayashi: He received his Ph. D. in Mechanical Engineering Department, the University of Tokyo in 1970. After completion his Ph.D. program, he has been a faculty member of Institute of Industrial Science, University of Tokyo, and currently is a Professor. His research interests are numerical analysis of turbulence, especially Large Eddy Simulation (LES), and particle imaging velocimetry (PIV) technique. He serves as the President to the Visualization Society of Japan (VSJ), President-elect to the Japan Society of Mechanical Engineers (JSME), and Executive Vice President to the Society of Automotive Engineer of Japan (JSAE).



Shigeru Murata: He received his BSc(Eng) degree in mechanical engineering from Kyoto Institute of Technology in 1982, MSc.(Eng.) degree in 1984 and Ph. D.(Eng.) degree in 1993 from Kyoto University. He started work at Kyoto Institute of Technology in 1984 after he got his MSc. (Eng.) degree, and is currently an Associate Professor in the Department of Mechanical and System Engineering at Kyoto Institute of Technology. His current research interests are focused on optical techniques for flow measurements and development of digital holography in mechanical engineering.



Koji Okamoto: He received his MSc (Eng) in Nuclear Engineering in 1985 from University of Tokyo. He also received his Ph.D. in Nuclear Engineering in 1992 from University of Tokyo. He worked in Department of Nuclear Engineering, Texas A&M University as a visiting associate professor in 1994. He has been working in the Nuclear Engineering Research Laboratory, University of Tokyo as an associate professor since 1993. His research interests are Quantitative Visualization, PIV, Holographic PIV, Flow Induced Vibration and Thermal-hydraulics in Nuclear Power Plant.



Shigeru Nishino: He graduated from Osaka University in 1983 and received his MSc(Eng) degree in Naval Architecture in 1985. He worked in Department of Marine System Engineering, Osaka Prefecture University from 1988 to 1999. He was awarded Ph. D.(Eng) degree in ship hydrodynamics, study on the three-dimensional separated flow around prolate spheroids and ships at incidence in 1990. He has been working as an Associate Professor in Kobe University of Mercantile Marine, Department of Maritime Science since 1999. His research interests are in the image measurement of flow field and the bio-fluid mechanics in fish-like propulsions.